4ICEGE Thessaloniki-GREECE 2007

4th International Conference on
Earthquake Geotechnical Engineering
June 25-28, 2007
Paper No. 1660

SMART BASE ISOLATION DESIGN INCLUDING MODEL UNCERTAINTY IN GROUND MOTION CHARACTERIZATION

Alexandros TAFLANIDIS [1], Jeffrey SCRUGGS[2] and James BECK[3]

ABSTRACT

A feedback controller design for smart base isolation systems is considered in this study. The control law is designed for optimal reliability, quantified as the probability, based on the available information, that the structural response will not exceed acceptable performance bounds. A realistic model for the stochastic representation of near-fault ground motions is adopted in the design stage. The variability of the ground motion is addressed by incorporating a probabilistic description for the uncertain model parameters. Stochastic simulation is used for the evaluation of the structural response. This simulation-based approach explicitly takes into account the non-linear characteristics of the structural response in the controller design process. The methodology is illustrated through application to the base isolated benchmark building with bilinear hysteretic bearings (e.g., lead-rubber bearings) and an array of regenerative force actuators (providing the control force).

Keywords: smart base isolation, stochastic ground motion, probabilistic model uncertainty.

INTRODUCTION

Over the last decade there has been a growing interest in the application of control technologies to civil structures, to reduce seismic risk, and many different strategies have been proposed for the design of smart forcing systems and feedback controllers to accomplish this goal (Spencer and Nagarajaiah 2003). Of these many approaches, smart base isolation systems have emerged as one of the more promising. One of the main challenges in controlling base isolated buildings has been the explicit consideration of the nonlinear behavior of the isolators in the controller design. Another challenge has been the development of forcing systems which yield efficient control of the dynamic response under near-fault ground motions. Such motions frequently include a strong longer period pulse that has important implications for flexible structures, such as base isolated systems (Hall et al. 1995). Proper characterization and study of their effects on engineering structures is currently an active research topic for both seismologists and earthquake engineers (Mavroeidis and Papageorgiou 2003).

A methodology is proposed here for design of feedback controllers which address both these challenges. The approach is applied to the base-isolated benchmark building (Narashiman et al. 2006). The controller is optimized based on reliability criteria, where the reliability of the system is quantified by the probability that the response will not exceed some acceptable performance bounds. In this context, uncertainty in the model parameters is treated through the incorporation of probabilistic description for them (Papadimitriou et al. 2001). Stochastic simulation is used for evaluation of the structural response, which allows for explicitly taking into account the non-linear characteristics of the base isolation system. Additionally, a stochastic model for the realistic description of near-fault ground motions is incorporated into the system model in the design stage.

[1] Ph.D candidate, Div. of Engr. & Appl. Sci., Caltech, Pasadena, USA, Email: taflanid@caltech.edu
[2] Assistant Professor, Dept. of Civil & Env. Engr., Duke University, Durham, USA.
[3] Professor, Div. of Engr. & Appl. Sci., Caltech, Pasadena, USA.

RELIABILITY-BASED STRUCTURAL CONTROL DESIGN

Since the knowledge about a system in engineering applications is never complete, the concept of reliability has been incorporated into engineering design as a means of explicitly taking into account system and excitation model uncertainties. In this context, the performance of a system is quantified by using probability as a measure of the plausibility of the occurrence of system failure, based on the available information (Papadimitriou et al. 2001). The motivation for the application of control technology to civil systems and the metrics by which the quality of such systems are judged ultimately stems from this concept of system reliability. The optimal strategy in structural control design should therefore be that which maximizes reliability. The design of controlled linear structural systems under stationary excitation, with reliability-based objectives and probabilistic model uncertainty has been extensively discussed in (Taflanidis et al. 2006). This methodology is extended here to nonlinear systems and non-stationary excitation.

Consider a controlled structural system, subjected to uncertain earthquake excitation. The system description is comprised of the mathematical model for the structure, augmented by dynamic models characterizing the sensor and actuator dynamics, the ground acceleration, the dynamic properties of the control law and so forth. Assume that the system properties depend on a set of h uncertain parameters and let the vector of these parameters be $\boldsymbol{\theta} \in \Theta$, where $\Theta \subset \mathbb{R}^h$ denotes the set of possible parameter values. The available knowledge about the values of these parameters is incorporated into the model by assigning a PDF $p(\boldsymbol{\theta})$ to them. The existence of non-parametric, unmodeled uncertainty is addressed by introducing a model prediction error ε, i.e. an error between the response of the actual system and the response of the model adopted for it (Beck and Katafygiotis 1998).

Let the adjustable parameters that define the control law be $\mathbf{K} \in K$ where K denotes the admissible design space. Then to design the controller we select $\mathbf{K}$ to give optimal reliability; i.e., minimal probability of structural failure. "Failure" is interpreted as the event that the response vector of the system, $\mathbf{z}(t)$, will exit a safe domain D_s within the duration of the excitation T. Vector $\mathbf{z}(t)$ is comprised of response quantities that are considered important for the system design, such as inter-story drifts, base shear or member forces. The failure threshold for these response variables, defining the boundary of the safe region, is designated as a bound on acceptable performance. Let $g(\boldsymbol{\theta},\mathbf{K})>0$ be the function defining the models failure; for example if $\mathbf{z}=[z_1 \ldots z_n]$ contains inter-story drifts, z_i, then an appropriate definition is $g(\boldsymbol{\theta},\mathbf{K})=\max(z_i/\beta_i)-1$, where β_i corresponds to the maximum allowable drift for the i^{th} story according to the designer's interpretation of acceptable performance. If $P_\varepsilon(.)$ is the cumulative distribution function (CDF) for the model prediction error ε, then the failure probability for a given $\mathbf{K}$ is expressed as (Taflanidis and Beck 2006):

$$P(F \mid \mathrm{K}) = P\left(\mathbf{z}(t) \notin D_s \text{ for some } t \in [0,T] \mid \mathbf{K}\right) = \int_{\Theta} P_\varepsilon(g(\boldsymbol{\theta},\mathbf{K}))\, p(\boldsymbol{\theta}) d\boldsymbol{\theta} \tag{1}$$

If no prediction error is assumed then $P_\varepsilon(.)$ in (1) is replaced by the indicator function $I_F(.)$, which is one if the system fails, i.e $g(\boldsymbol{\theta},\mathbf{K})>0$, and zero if not and thus expresses a binary distinction for the system performance. Therefore, the influence of the prediction error in this formulation can be equivalently considered as introduction of a function that incorporates a preference for the system performance, expressed through the value $P_\varepsilon(g(\boldsymbol{\theta},\mathbf{K}))$ (see also comparison in Figure 5(c) later on).

The integral in (1) can rarely be calculated analytically, especially for complex systems, and so it is often estimated by stochastic simulation using a finite number N of random samples of $\boldsymbol{\theta}$, drawn from $p(\boldsymbol{\theta})$. In this context, the evaluation of the system's response, i.e. calculation of $g(\boldsymbol{\theta},\mathbf{K})$, can also be performed based on a computer simulation - rather than approximated analytically as in (Taflanidis et al. 2006). The failure probability and the optimal reliability controller are then

$$\hat{P}\left(F \mid \mathbf{K}\right) = 1/N \cdot \sum_{i=1}^{N} P_\varepsilon(g(\boldsymbol{\theta}_i,\mathbf{K})), \quad \mathbf{K}^* = \arg\min_{\mathbf{K} \in K} \hat{P}\left(F \mid \mathbf{K}\right) \tag{2}$$

The optimization in (2) is challenging. First of all, the evaluation for $P(F|\mathbf{K})$ involves an unavoidable estimation error; the existence of this error contrasts with classical deterministic optimization where it is assumed that one has perfect information. Furthermore each evaluation of the objective function in (2) requires typically a substantial computational effort. The highly efficient framework presented recently by (Taflanidis and Beck 2006) is used in this study to perform this controller optimization. More details for this framework are not presented here because it is not directly connected to the design methodology discussed (any stochastic optimization algorithm could be alternatively used).

STOCHASTIC MODEL FOR NEAR-FAULT GROUND MOTIONS

This reliability-based framework requires a probabilistic model for describing the stochastic input, i.e. the earthquake excitation. Contrary to linear control methodologies, for which such models have to be simple, simulation-based reliability design allows for consideration of more complicated descriptions for the ground motion. Two desirable characteristics for the models used for this purpose are: (i) parameters with well defined physical meaning which can be treated in a realistic probabilistic framework, and (ii) small computational effort to simulate a sample of the excitation (since a large number of simulations will be typically needed for the controller optimization). The model used in this study is based on the methodologies presented by (Mavroeidis and Papageorgiou 2003) and (Boore 2003). These methodologies, which were initially developed for generating synthetic ground motions, are reinterpreted here to form a stochastic model for the earthquake excitation. The low-frequency (long period) and high-frequency components of the ground motion are independently modeled, according to these methodologies, and then combined to form the acceleration time history.

High-frequency component

The fairly general, point-source stochastic method (Boore 2003) is selected for modeling the higher-frequency (>0.1-0.2 Hz) component of ground motions. The stochastic method is based on a parametric description of the ground motion's radiation spectrum $A(f;M,r)$ which is expressed as a function of the frequency, f, for specific values of the earthquake magnitude, M, and epicentral distance, r. This spectrum consists of many factors which account for the spectral effects from the source (source spectrum) as well as propagation through the earth's crust. The duration of the ground motion is addressed through an envelope function $e(t;M,r)$, which again depends on M and r. These frequency and time domain functions, $A(f;M,r)$ and $e(t;M,r)$, completely characterize the model. More details on them are provided in Appendix A. Particularly, the two-corner point-source model by (Atkinson and Silva 2000) is selected for the source spectrum because of its equivalence to finite fault models. This equivalence is important because we intend to describe near-fault motions and adaptation of a point-source model might not efficiently address the proximity of the site to the source (Mavroeidis and Papageorgiou 2003). The spectrum adopted here has been reported (Atkinson and Silva 2000) to efficiently address this characteristic.

The time-history (output) for a specific event magnitude, M, and source distance, r, is obtained according to this model by modulating a white noise sequence $\mathbf{Z}_w$ (input) through the following steps: (i) the sequence $\mathbf{Z}_w$ is multiplied by the envelope function $e(t;M,r)$; (ii) this modified sequence is then transformed to the frequency domain; (iii) it is normalized by the square root of the mean square of the amplitude spectrum; (iv) the normalized sequence is multiplied by the radiation spectrum $A(f;M,r)$ and finally (v) it is transformed back to the time domain to yield the desired acceleration time history.

Low-frequency component

For describing the pulse characteristic of near-fault ground motions, the simple analytical model developed by (Mavroeidis and Papageorgiou 2003) is selected. This model is based on an empirical description of near-fault ground motions and has been calibrated using a large number of actual near-field ground motion records from all over the world. According to it, the pulse component (due to forward directivity and permanent offset effects) of near-fault motions is described through the following expression for the ground motion velocity pulse:

$$V(t)=\frac{A}{2}\left[1+\cos\left(\frac{2\pi f_p}{\gamma}(t-t_o)\right)\right]\cos\left[2\pi f_p(t-t_o)+\nu\right]\ ,\ t\in\left[t_o-\frac{\gamma}{2f_p},t_o+\frac{\gamma}{2f_p}\right];\ =0\ \text{otherwise} \qquad (3)$$

where A, f_p, v, γ and t_o describe the signal amplitude, prevailing frequency, phase angle, oscillatory character (i.e., number of half cycles) and time shift to specify the epoch of the envelope's peak, respectively. Note that all parameters have an unambiguous physical meaning. Selection of the last three parameters will be discussed later. The first two may be chosen according to the guidelines provided by (Somerville 1998) for the pulse frequency, $\log_{10}f_p$=3-0.5M_w, and the peak ground velocity (PGV), $\log_{10}$PGV=0.5M_w-1-0.5$\log_{10}R$, of near-fault ground motions. In these expressions M_w is the seismic moment and R the closest distance from the fault. Both of these parameters can be calculated based on the values for the moment magnitude and the distance from the source (see Appendix A).

Model of ground motion

The stochastic model for near-fault ground motions is finally established by combining the above two components. The input to the model is the white noise sequence $\mathbf{Z}_w$ and the model parameters consist of the seismological parameters M and r and the additional parameters for the velocity pulse, v and γ. The selection of all these parameters will be discussed later. The following procedure, which is equivalent to the methodology in (Mavroeidis and Papageorgiou 2003), describes the model:

(1) Apply the stochastic method to generate an acceleration time history.
(2) Generate a velocity time history for the near-field pulse using equation (3). The pulse is shifted in time to coincide with the peak of the envelope $e(t;M,r)$. This defines the value of the time shift parameter t_o. Differentiate the velocity time series to obtain an acceleration time series.
(3) Calculate the Fourier transform of the acceleration time histories generated in steps 1 and 2.
(4) Subtract the Fourier amplitude of the time series generated in step 2 from the spectrum of the series generated in 1.
(5) Construct a synthetic acceleration time history so that its Fourier amplitude is the one calculated in step 4 and its Fourier phase coincides with the phase of the time history generated in step 2.
(6) Finally superimpose the time histories generated in steps 2 and step 5.

Figures 1(a) shows functions $A(f;M,r)$ and $e(t;M,r)$ for different values of M and r=15 km. It can be seen that as the moment magnitude increases the duration of the envelope function also increases and the spectral amplitude becomes larger at all frequencies with a shift of dominant frequency content towards the lower-frequency regime. Figures 1(b) and 2 illustrate some key points for a sample synthetic near-fault ground motion for values M=6.7, r=5km, γ=1.8 and v=π/6. Figure 1(b), includes the radiation spectrum $A(f;M,r)$ and the Fourier amplitude of the sample ground motion generated according to the stochastic method. The acceleration and velocity time histories of the synthetic ground-motion are shown in Figure 2. The difference between the ground motions generated by the stochastic method and the final time history are evident in this figure (in terms of the velocity pulse).

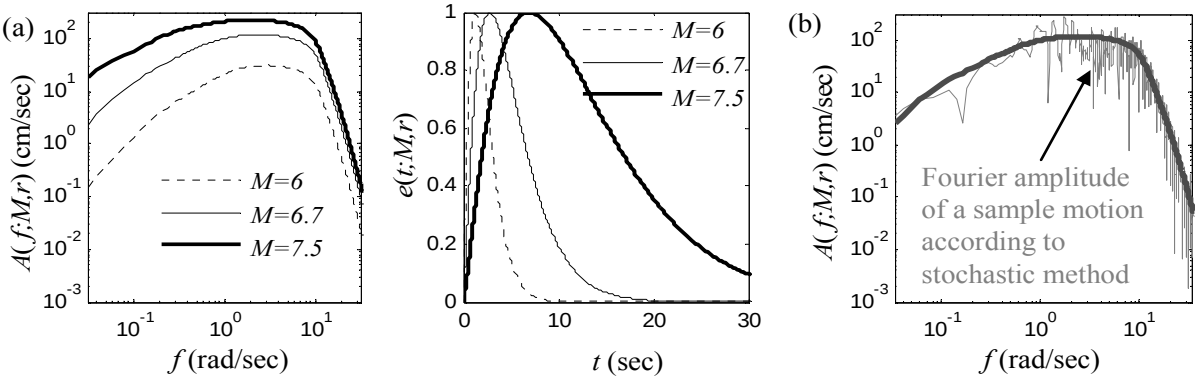

Figure 1. (a) Radiation spectrum and envelope function for various M and r=15 km and (b) radiation spectrum and Fourier amplitude of a sample ground motion for M=6.7, r=5 km.

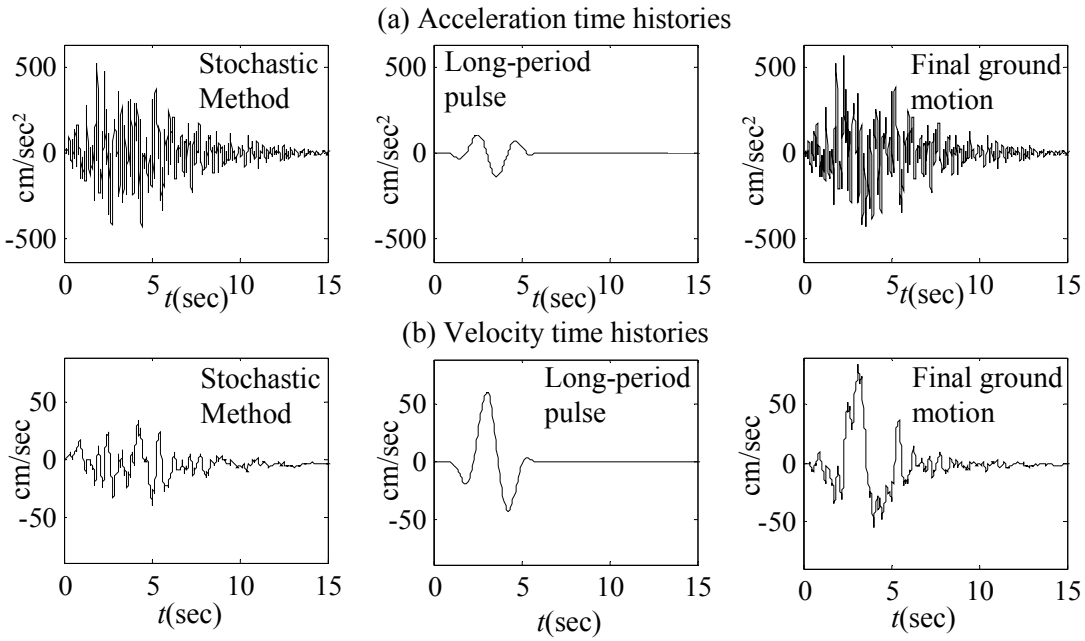

Figure 2. Sample near-fault ground motion: acceleration and velocity time histories for (i) stochastic method (ii) long period pulse and (iii) final ground motion

BENCHMARK BASE-ISOLATED STRUCTURE WITH REGENERATIVE ACTUATORS

The benchmark model (Narashiman et al. 2006) is a base-isolated structure with n_f=8 floors. Stories 1-6 have a torsionally asymmetric L-shaped plan while the higher floors have a rectangular plan. The superstructure is a linear elastic system resting on a concrete base. The base and floor slabs are assumed to be infinitely rigid in plane, and are modelled by three master degrees of freedom located at the centres of mass of each floor. Below the base, the isolation system consists of a variety of 92 isolation bearings. In this study, the isolators are selected as 31 linear elastomeric rubber bearings and 61 lead rubber-rubber bearings (Figure 3(b)). The linear bearings are modelled with linear stiffness and linear viscous damping. The lead-rubber bearings are modelled with bilinear hysteretic stiffness, using the Bouc-Wen model as discussed in (Narashiman et al. 2006) to take into account biaxial interaction, and linear viscous damping. The properties of the isolators are the same as in (Erkus and Johnson 2006). Noisy acceleration measurements are available at the center of mass of each floor level and the base for control applications. Appendix B provides a brief description of the mathematical model for the benchmark structure.

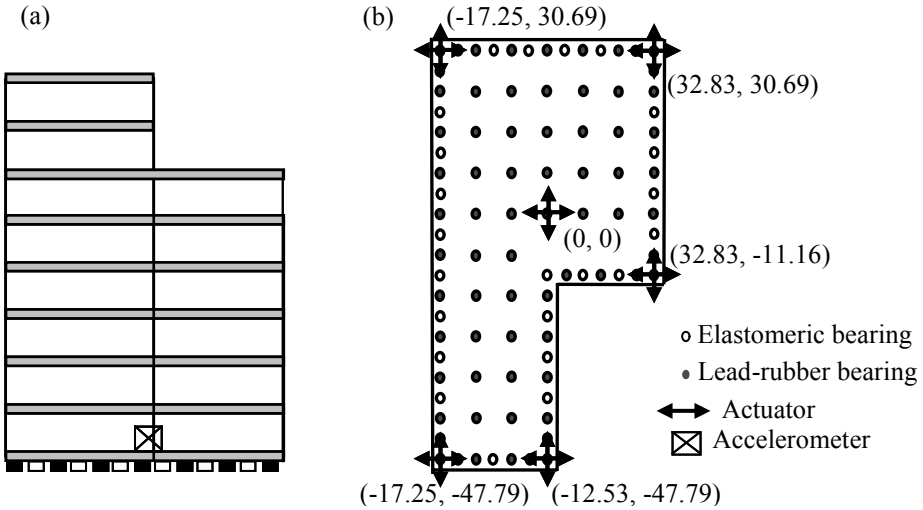

Figure 3. (a) Side view and (b) base plan of the benchmark structure

In this study a Regenerative Force Actuation (RFA) network is implemented at the base level for the protection of the benchmark structure. RFA networks (Scruggs and Iwan 2005) are an extension of semiactive devices, in which mechanical energy is first converted to electrical energy, and is then dissipated in a controllable resistive network. Their mode of operation is similar to many other semiactive systems; it can be viewed as providing controllable viscous damping. However, these networks have a unique advantage in that if two or more devices are used to control a structure (Figure 4(a.i)), their associated electronics may be connected such that electrical power can be transmitted from one actuator to another (Figure 4(a.ii)). Thus, in addition to providing local dissipation (as do semi-active actuators), it is possible to transmit energy between remote locations in a structure. The network, as a whole, must always dissipate energy, which imposes a constraint on the system forcing capabilities. Consider a network of m actuators and define $\mathbf{f} = [f_1 \ldots f_m]^T$ as the vector of actuator forces. Define $\mathbf{v} = [v_1 \ \ldots \ v_m]^T$ as the corresponding vector of relative actuator velocities. Let c_{ci} be the maximum effective viscous damping of each device (related to electrical characteristics) and define the matrix $\mathbf{C}_c$=diag[$c_{c1} \ldots c_{cm}$]. The velocity-dependent force constraints for the device system operating in regenerative mode or semi-active mode (i.e, without connecting the electrical networks of different actuators) are (Scruggs et al. 2007):

$$\text{Regenerative}: \mathbf{f}^T \mathbf{C}_c^{-1} \mathbf{f} + \mathbf{f}^T \mathbf{v} \le 0, \qquad \text{Semiactive: } f_i \in [-c_{ci} v_i, 0] \Leftrightarrow c_{ci}^{-1} f_i^2 + f_i v_i \le 0 \tag{4}$$

These feasible force regions are illustrated in Figure 4(b) for a two-actuator system. The regenerative constraint is less restrictive than the semiactive constraint because a single constraint is imposed on the entire network, whereas for semiactive systems the *same* constraint is imposed on *each device separately*. Note that, like semi-active devices, the energy required for operation of the electromechanical actuators in the RFA network is only that required for the sensory and intelligence systems, which, contrary to the requirements of fully-active system, can be provided by a small local power supply. This feature makes them an appropriate device for structural control applications, considering the inherent vulnerability of external power supplies in the event of an earthquake.

In this study, an array of six regenerative force actuators is considered in each direction, working in tandem with the isolation system. The position of the actuators with respect to the center of mass of the base is shown in Figure 3(b). In this configuration, energy is transmitted between the actuators at different locations in the base, as well as between the two translational directions of motion. The maximum viscosity of all actuators is set to 1150 kN sec/m. This choice implies that the total maximum capability for the RFA network in both translational directions is equal to 10% critical damping and corresponds to a reasonable selection, considering current actuator capabilities.

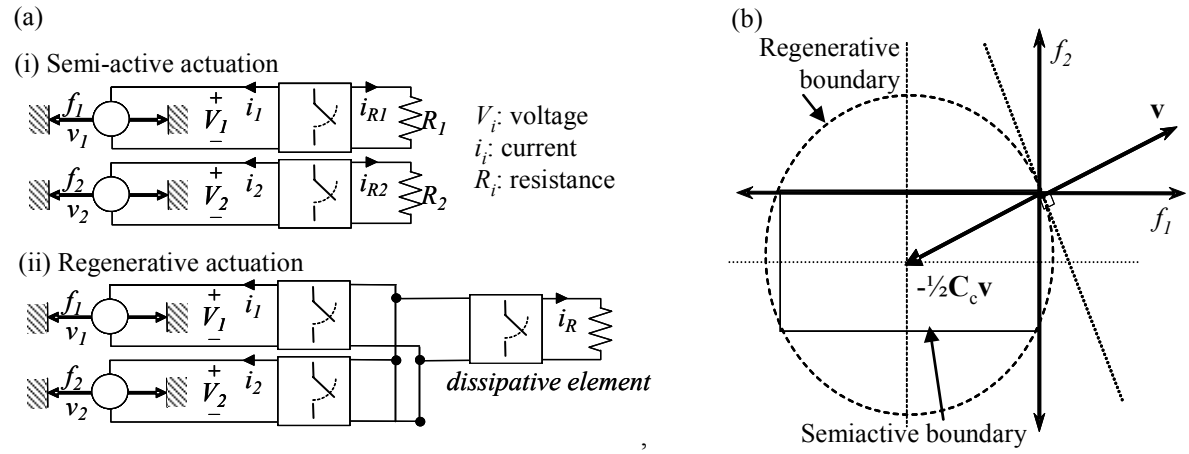

Figure 4. (a) Electromechanical actuation and (b) feasible force region for regenerative and semiactive two actuator system

The control law is assumed to be of a "skyhook" form; i.e., the total control forces at the center of mass of the base are determined as a feedback function of the absolute velocities of the respective degrees of freedom. The control law in this case consists, therefore, of a three-dimensional feedback gain vector $\mathbf{K} \subset \mathbb{R}^3$. The force distribution on the different actuators is decided as in (Scruggs et al. 2006), so that the minimum control effort is required (more details on Appendix B). Absolute velocity measurements are obtained by filtering the accelerometer measurements through a second order filter, as suggested in (Narashiman et al. 2006). At any time that the desired linear feedback control forces violate (4), the magnitude of the control force vector is scaled radially to the circular boundary given by the regenerative constraint.

CONTROLLER DESIGN FOR BENCHMARK STRUCTURE

The control law is optimized using the reliability-based design framework and the near-fault ground motion model presented earlier. The vector **z** of performance quantities for the controller design consists of (a) inter-story drifts of all floors, (b) base displacement at the outermost corner and (c) absolute accelerations at the center of mass of all floor and the base. Failure is defined for the system if any of these quantities exceeds its respective threshold. The failure thresholds are chosen to be, respectively, 0.22% of the story height, 0.5m, which is comparable to the clearance adopted in many base-isolated buildings (Hall et al. 1995), and 0.4*g*. The response of the base-isolated structure is evaluated through a computer-based simulation using the SIMULINK toolbox of MATAB. This way the non-linear characteristics of the isolators are explicitly addressed for controller design.

The parameters adopted for the stochastic method (as described in Appendix A) are: radiation pattern R_{Φ}=0.55, rock density ρ_s=2.8 g/cm^3 and shear-wave velocity β_s=c_Q=3.5 km/sec; anelastic attenuation factor $Q(f)=180f^{0.45}$ (selected for the region of California according to (Atkinson and Silva 2000)) and geometrical spreading function $Z(R)=1/R$ for distances R<40km. The diminution is expressed through combination of both f_{max} and k_o filters with values f_{max}=10 rad/sec and κ_o=0.03. The latter selection is a compromise between regional estimates for California that typically range from about 0.02 to 0.04 (Atkinson and Silva 2000). Site amplification is chosen for generic rock sites (Boore and Joyner 1997). The parameters for the envelope function $e(t;M,r)$ are λ=0.2, η=*0.05* (as suggested in (Boore 2003)) and the duration is selected as $T_w=0.05R+0.5f_a$.

The variability of the excitation is addressed by assigning a PDF to the uncertain seismological (moment magnitude, M and epicentral distance, r) and ground motion model parameters. The latter include (i) the parameters that have already been described earlier, i.e. phase angle, v and oscillatory character, γ, for the velocity pulse, as well as (ii) two additional parameters that address the bi-directional characteristics of the ground motion. These parameters are (a) a reduction factor, A_n, for the fault-parallel component of the ground motion, and (b) the angle, δ, that the ground motion impacts the structure. Note that the base isolation structure is a torsionally asymmetric building and thus its dynamic performance needs to be evaluated under bi-directional loading. Since there is no well-defined method for modeling the characteristics of the fault-parallel component of near-fault ground motions using the stochastic method, an approximation based on engineering judgment is adopted. The same model is used for both fault parallel and fault normal components but a reduction factor is introduced for the fault parallel component. Also, the white-noise sequences that are used to generate the time histories for the two components are chosen to be different. This agrees with the observation (Jangid and Kelly 2001) that the two orthogonal components of near-fault motions have incoherent characteristics.

We consider only severe seismic events, so the uncertainty in M is modeled by the Gutenberg-Richter relationship, $p(M)=\beta\exp(-\beta M)/[\beta\exp(-\beta M_{min})-\beta\exp(-\beta M_{max})]$, truncated on the interval $[M_{min}, M_{max}]=[6.5, 7.7]$, with seismicity factor $\beta=1.2\log_e(10)$, which is a typical value. For the uncertainty in the event location, earthquakes are assumed to be equally likely to occur in a circular area of radius r_{max}=20km centered at the structural site, leading to a triangular distribution for r on

[0, 20] km and a uniform distribution for δ on [-π, π]. The selection for r_{max} and M_{min} was based on the observation that events at larger distances or of smaller magnitude could rarely lead to failure of the system and thus have no significance for the controller design.

The probability distribution for the velocity pulse characteristics are selected as uniform on [-π/2, π/2] for v, and Gaussian with mean 1.8 and standard deviation 0.4 for γ. These choices are based on the values reported by (Mavroeidis and Papageorgiou 2003) when calibrating their model to a database of near-fault ground motions. The uncertainty in the reduction factor for the fault parallel component of the ground motion is modeled by a uniform distribution on the range [0.6, 0.9]. This type of distribution is chosen to reflect that there is little available information for the relationship between the two orthogonal components of the ground motion. The range is selected according to engineering judgment. Finally, the model prediction-error is assumed to be log-normally distributed with median one and logarithm of standard deviation 0.06. This selection coincides with the common probability model chosen in performance-based design methodologies for the engineering demand parameters (such as maximum drifts). Figure 5 shows the selected distribution functions for some of the above parameters. In Figure 5(c) the dotted line corresponds to the indicator function $I_F(.)$ which would be the function evaluating the system performance if ε=0 was assumed. The comparison to $P_\varepsilon(.)$ illustrates clearly the influence of the model prediction error (as discussed earlier).

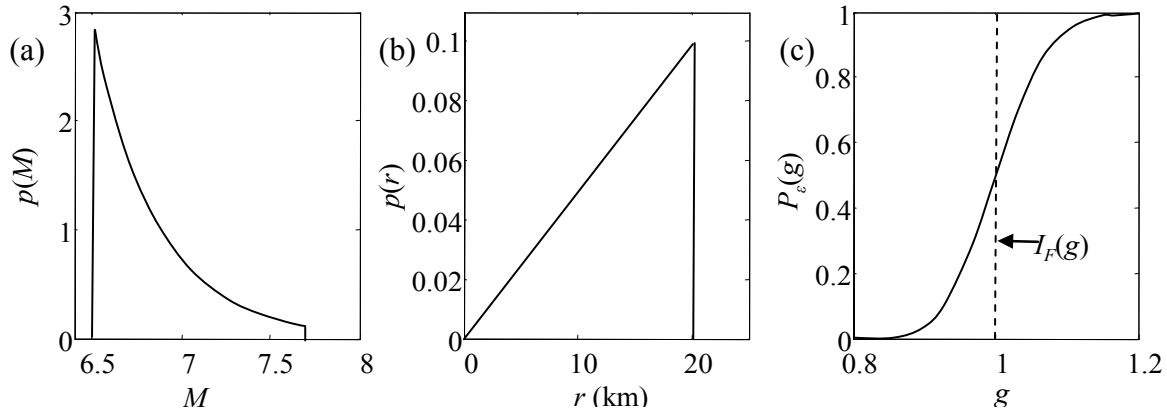

Figure 5. (a) PDF for *M*, (b) PDF for r and (c) CDF for ε

EVALUATION OF CONTROLLER PERFORMANCE FOR BENCHMARK STRUCTURE

Under the uncertainty framework considered, the probability of failure of the base-isolated structure, given a severe seismic event, is 0.27 without the control system and 0.13 under optimal design with the RFA network. This indicates that the RFA network contributes significantly in increasing structural reliability. The control design is further evaluated through the seven earthquakes suggested in (Narashiman et al. 2006) by the following performance indices (all normalized by the performance of the uncontrolled structure); J_1: peak inter-story drift, J_2: peak base displacement J_3: peak absolute acceleration at center of mass and J_4: peak base shear. For all earthquakes the fault normal and fault parallel component are considered to act in both perpendicular directions (x and y) and the worst case response is presented here. Results are presented in Table 1. Some indicative time-histories are shown in Figure 6.

Table 1: Performance indices for the controller evaluation

	Newhall	Sylmar	El Centro	Rinaldi	Kobe	Jiji	Erzikan
J_1	0.878	0.980	0.990	1.006	0.922	0.793	0.809
J_2	0.926	0.802	0.740	0.939	0.708	0.703	0.727
J_3	0.932	0.961	1.007	1.052	0.930	0.863	0.892
J_4	0.925	0.888	1.013	0.980	0.878	0.850	0.868

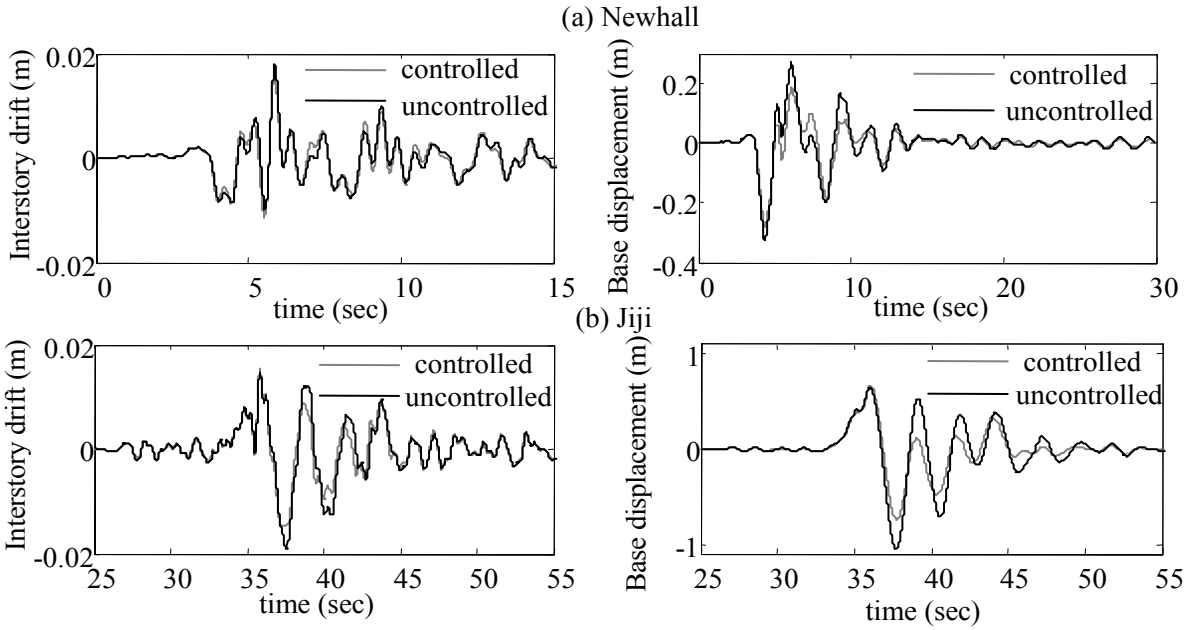

Figure 6. Uncontrolled and controlled time history response for base displacement and inter story drifts for (a) Newhall and (b) Jiji earthquakes (worst case response is presented)

The results show that the control application improves the dynamic response of the system over most performance quantities. The reduction in the response is greatest for the base displacement and smallest for absolute accelerations. This is a direct result of the criteria that were set in the design stage (displacement quantities were given greater importance than acceleration) as well as the fact that the control force is applied in the base level (so base displacement is easier to regulate than inter-story drifts). It is interesting to note that for most earthquakes, reduction of the peak absolute acceleration is also achieved, even though it is only a small percentage. This is an important accomplishment since the reduction of both displacement *and* absolute acceleration quantities is recognized as a difficult challenge in semi-active control of base-isolated structures.

The significance of the stochastic ground motion model in the controller design is partially assessed by a performance comparison to an alternative design. This alternative design adopts a stochastic model for the ground motion that does not include the near-fault, long-period component (so the excitation is described solely by the stochastic method for the controller optimization stage). Such a representation of the ground motion is similar to the models adopted in most structural control methodologies for stochastic characterization of the earthquake excitation (which commonly involve a Kanai-Tajimi type of spectrum). Still the design considered here is different than those methodologies because they assume a linearized system and a deterministic selection for the model parameters. Results for the alternative controller are shown in Table 2. Comparing the performance in Tables 1 and 2, it is evident that the original design provides overall a better and more robust performance. The methodology used for the alternative design fails to take into account near-fault characteristics of the ground motion. Since the excitations used to evaluate the favorability of the controller include such characteristics, the performance is worse. This observation stresses the importance of using a model for the ground motion that can accurately describe potential future ground motions.

Table 2: Performance Indices for the alternative controller evaluation

	Newhall	Sylmar	El Centro	Rinaldi	Kobe	Jiji	Erzikan
J_1	0.898	1.006	1.092	1.167	0.967	0.824	0.878
J_2	0.921	0.795	0.778	0.951	0.681	0.757	0.727
J_3	0.967	1.097	1.027	1.157	1.077	0.903	0.934
J_4	0.924	0.838	1.136	0.977	0.885	0.837	0.845

CONCLUSIONS

The controller design for base-isolated structures was discussed in this paper. A methodology was illustrated that uses reliability criteria to access the favorability of different controllers and allows for explicitly taking into account (a) nonlinear characteristics for the system, and (b) model uncertainty. A realistic model was presented for the stochastic representation of near-fault ground motions. The uncertainty regarding the model parameters was addressed by assigning PDFs to them. These probability models incorporate the available knowledge into the model of the system. As little information is available in the literature for a probabilistic interpretation of ground-motion models, the choice of PDFs was based on the judgment of the authors. Further research in this direction would greatly improve the efficiency of the methodology presented here. Still, the design method presented allows for consideration of realistic models for the stochastic description of ground motion. The effectiveness of the method depends on the ability of the model adopted to represent future ground motions. If the representation is adequate and the uncertainty about the model parameters is quantified properly, the proposed methodology can provide significant improvement of the structural reliability.

Application to the benchmark base-isolated building was discussed. A regenerative actuator network was considered at the base level that allows for energy transmission between different locations and directions of motion. The results illustrate significant reduction in important response quantities that shows the efficiency of both the controller design methodology and the capabilities of the regenerative actuators. More detailed quantification of the uncertainty for the ground motion model parameters, which will be possible when a specific site is considered, can further improve this efficiency. Comparison to an alternative controller design was also discussed. The comparison illustrated the importance of adopting a model for the excitation that adequately describes the main characteristics of potential future ground motions.

APPENDIX A

A thorough review of the stochastic method for generation of synthetic ground motions is presented by (Boore 2003). The characteristics for the functions $A(f;M,r)$ and $e(t;M,r)$ are briefly summarised here. The total spectrum $A(f;M,r)$ for the acceleration time history may be expressed as a product of the source, $E(f;M)$, path, $P(f;\mathrm{r})$, and site, $G(f)$, contributions:

$$A(f;M,r) = (2\pi f)^2 E(f;M)P(f;r)G(f) \tag{5}$$

The source spectrum is given by:

$$E(f;M) = CM_w S(f;M) \text{ with } S(f;M) = \left[\frac{1-e}{1+\left(f/f_a\right)^2} + \frac{e}{1+\left(f/f_b\right)^2}\right] \tag{6}$$

where the displacement source spectrum $S(f;\mathrm{M})$ described above is the two-corner point-source model developed by (Atkinson and Silva 2000) for ground motions in California (see (Boore 2003) for other models for $S(f;\mathrm{M})$). For this spectrum the lower and upper frequencies are given by $\log_{10} f_a$=2.181-0.496M and $\log_{10} f_b$=2.41-0.408M, respectively, and e is a weighting parameter described by the expression $\log_{10} e$=0.605-0.255M. In equation (6) M_w is the seismic moment (in dyn-cm) which is connected to the moment magnitude by the relationship $\log_{10} M_w$=1.5(M+10.7). The constant C is given by $C=R_\Phi VF/(4\pi R_o \rho_s \beta_s)$, where R_Φ is the radiation pattern, usually averaged over a suitable range of azimuths and take off angles , $V=1/\sqrt{2}$ represents the partition of total shear-wave velocity into horizontal components, F=2 is the free surface amplification, ρ_s and β_s are the density and shear-wave velocity in the vicinity of the source, and R_o is a reference distance, set to 1km.

The path effect, $P(f;r)$, is given by the multiplication of the geometrical spreading and anelastic attenuation $P(f;r)=Z(r)\exp[-\pi f \cdot R/(Q(f)\cdot c_Q)]$, where $Q(f)$ is a regional attenuation function, c_Q is the seismic velocity used in the determination of $Q(f)$, $Z(r)$ is the geometrical spreading function and $R=[h^2+r^2]^{1/2}$ is the radial distance from the earthquake source to the site, with $\log_{10}h=0.15M-0.05$ (Atkinson and Silva 2000) representing a moment-dependent, nominal "pseudo-depth". The site effect, $G(f)$, is given by the multiplication of a high-frequency diminution $D_m(f)$ and an amplification factor $A_m(f)$, $G(f)=A_m(f)D(f)$. The diminution may be expressed by the k_o filter $D(f)=\exp(-\pi\kappa_o f)$ or the f_{max} filter $D(f)=[1+(f/f_{max})^8]^{-1/2}$ or a combination of both (Boore 2003). The amplification factor may be described through the empirical curves given in (Boore and Joyner 1997).

Finally, the envelope function for the earthquake excitation is represented by

$$e(t;M,r) = a\left(t/t_n\right)^b \exp\left(-c(t/t_n)\right) \tag{7}$$

where a, b and c are chosen so that $e(t;M,r)$ has a peak equal to unity when $t=\lambda t_n$ and $e(t;M,r)=\eta$ when $t=t_n$. The equations for these parameters are $b=-\lambda\ln(\eta)/[1+\lambda(\ln(\lambda)-1)]$, $c=b/\lambda$ and $a=[\exp(1)/\lambda]^b$. The time t_n is given by $t_n=2T_w$ where T_w is the duration of the ground motion, expressed as a sum of a path dependent (typically chosen as $0.05R$) and a source dependent component (typically chosen as a fraction of $1/f_a$).

APPENDIX B

A brief description of the mathematical model for the benchmark structure is presented here. The stuperstructure is assumed to be a linear system with mass, damping and stiffness matrices $\mathbf{M}_s$, $\mathbf{C}_s$, and $\mathbf{K}_s$. Also $\mathbf{M}_b$, $\mathbf{C}_b$ and $\mathbf{K}_b$ denote the mass and damping matrices for the base and the stiffness matrix of the linear isolators, respectively. The differential equation for the coordinate vector $\mathbf{p}$ (consisting of lateral and rotational displacements for each floor and the base) can be expressed as:

$$\begin{bmatrix} \mathbf{M}_s & \mathbf{M}_s\mathbf{R} \\ \mathbf{R}^T\mathbf{M}_s & \mathbf{R}^T\mathbf{M}_s\mathbf{R}+\mathbf{M}_b \end{bmatrix}\ddot{\mathbf{p}} + \begin{bmatrix} \mathbf{C}_s & \mathbf{0}_{3n_f\times 3} \\ \mathbf{0}_{3n\times 3_f} & C_b \end{bmatrix}\dot{\mathbf{p}} + \begin{bmatrix} \mathbf{K}_s & \mathbf{0}_{3n_f\times 3} \\ \mathbf{0}_{3n\times 3_f} & \mathbf{K}_b \end{bmatrix}\mathbf{p} = \begin{bmatrix} \mathbf{0}_{3n_t\times 3} \\ \mathbf{I} \end{bmatrix}\mathbf{u}_f + \begin{bmatrix} \mathbf{0}_{3n_t\times 3} \\ \mathbf{I} \end{bmatrix}\mathbf{F}_{is} + \begin{bmatrix} \mathbf{M}_s\mathbf{R} \\ \mathbf{R}^T\mathbf{M}_s\mathbf{R}+\mathbf{M}_b \end{bmatrix}\begin{bmatrix} \ddot{\mathbf{x}}_g \\ 0 \end{bmatrix} \tag{8}$$

where $\ddot{\mathbf{x}}_g \in \Re^2$ is the acceleration of the ground in the x and y directions and $\mathbf{R}$ is the $3n_f\times 3$ matrix of earthquake influence coefficients. Vector $\mathbf{u}_f$ contains the total control on the base in the x and y directions and the total control torque about the base center of mass. This vector and the vector of forces produced by each individual device, $\mathbf{f}$, are related by

$$\mathbf{u}_f=\mathbf{R}_c\mathbf{f} \text{ where } \mathbf{R}_c=\begin{bmatrix} \mathbf{r}_c^1 & \ldots & \mathbf{r}_c^{n_c} \end{bmatrix}, \text{ with } \mathbf{r}_c^i=\begin{cases} \begin{bmatrix} 1 & 0 & -y_c^i \end{bmatrix}^T & \text{(actuator in the } x\text{-direction)} \\ \begin{bmatrix} 0 & 1 & x_c^i \end{bmatrix}^T & \text{(actuator in the } y\text{-direction)} \end{cases} \tag{9}$$

Note that in the controller formulation considered in this study the total force vector $\mathbf{u}_f$ is designated as a feedback function of the response measurements. The forces on each actuator are then decided, based on the value of $\mathbf{u}_f$. Since there are 12 actuators (not all aligned with each other), equation $\mathbf{u}_f=\mathbf{R}_c\mathbf{f}$ has infinite solutions for $\mathbf{f}$, given $\mathbf{u}_f$ ($\mathbf{R}_c$ is rank three and therefore has a nontrivial nullspace). An optimum force distribution to the individual actuators may be derived by using the right generalized inverse of $\mathbf{R}_c$, $\mathbf{T}=\mathbf{R}_c^T(\mathbf{R}_c\mathbf{R}_c^T)^{-1}$. This choice produces the minimum-Euclidean-norm for $\mathbf{f}$ given $\mathbf{u}_f$.

Vector $\mathbf{F}_{is}$ in (8) contains the total forces produced by the nonlinear hysteretic isolators at the base center of mass. A relationship similar to (9) holds between $\mathbf{F}_{is}$ and the force provided by each individual isolator in each direction (considering biaxial interaction).

If the earthquake input is described by the ground motion model presented earlier then, $\ddot{\mathbf{x}}_g = \begin{bmatrix} \sin\delta & \cos\delta \\ \cos\delta & \sin\delta \end{bmatrix} \begin{bmatrix} \ddot{x}_{gn} \\ \ddot{x}_{gp} \end{bmatrix}$, where $\ddot{x}_{gn}$ and $\ddot{x}_{gp}$ are the fault-normal and fault-parallel components of the ground motion and δ is the angle the excitation impacts the structure.

REFERENCES

Atkinson, GM., and Silva, W., "Stochasit modeling of Calfornia ground motions," Bulletin of the Seismological Society of America, 90(2), 255-274, 2000.

Beck, JL., and Katafygiotis, LS., "Updating models and their uncertainties. I: Bayesian statistical framework," Journal of Engineering Mechanics, 124(4), 455-461, 1998.

Boore, DM., "Simulation of ground motion using the stochastic method," Pure applied Geophysics, 160, 635-676, 2003.

Boore, DM., and Joyner, WB., "Site amplifications for generic rock sites," Bulletin of the Seismological Society of America, 87, 327-341, 1997.

Erkus, B., and Johnson, EA., "Smart base isolated benchmark building Part III: a sample controller for bilinear isolation," Journal of Structural Control and Health Monitoring, 13, 605-625, 2006.

Hall, FF., Heaton, TH., Halling, MW., and Wald, DJ., "Near-source ground motion and its effects on flexible buildings," Earthquale Spectra, 11(4), 569-605, 1995.

Jangid, RS., and Kelly, JM., "Base isolation for near fault motions," Earthquake Engineering and Structural Dynamics, 30, 691-707, 2001.

Mavroeidis, GP., and Papageorgiou, AP., "A mathematical representation of near-fault ground motions," Bulletin of the Seismological Society of America, 93(3), 1099-1131, 2003.

Narashiman, S., Nagarajaiah, S., Johnson, EA., and Gavin, HP., "Smart base isolated benchmark building part I: Problem definition," Journal of Structural Control and Health Monitoring 13(2-3), 573-588, 2006.

Papadimitriou, C., Beck, JL., and Katafygiotis, LS., "Updating robust reliability using structural test data," Probabilistic Engineering Mechanics, 16, 103-113, 2001.

Scruggs, JT., and Iwan, WD., "Structural Control Using Regenerative Force Actuation Networks," Journal of Structural Control and Health Monitoring 12, 25-45, 2005.

Scruggs, JT., Taflanidis, AA., and Beck, JL., "Reliability-based control optimization for active base isolation systems, " Journal of Structural Control and Health Monitoring, 13, 705-723, 2006.

Scruggs, JT., Taflanidis, AA., and Iwan, WD., "Nonlinear stochastic controllers for semiactive and regenerative systems with guaranteed quadratic performance bounds. Part I-State Feedback Control," Journal of Structural Control and Health Monitoring, in press, 2007.

Somerville, P., "Development of an improved representation of near-fault ground motions," SIMP98-CDMG, 1-20, 1998.

Spencer, BF., Jr., and Nagarajaiah, S., "State of the Art in Structural Control," ASCE Journal of Structural Engineering, 129(7), 845-856, 2003.

Taflanidis, AA., and Beck, JL., "Reliability-based optimal design by efficient stochastic simulation," 5th international conference on computational stochastic mechanics, 14-16 June, 2006.

Taflanidis, AA., Scruggs, JT., and Beck, JL., "Reliability-based performance objectives and probabilistic model uncertainty in optimal structural control," 4th World Conference on Structural Control and Monitoring, 11-13 July, 2006.